MRS Advances (2023) 8:201–206
https://doi.org/10.1557/s43580-023-00511-7

ORIGINAL PAPER

Effect of the addition of Al_2O_3, ZnO and TiO_2 on the crystallization behavior, thermal and some physical properties of lead borate glasses

Yu. S. Hordieiev[1] · A. V. Zaichuk[1]

Received: 17 December 2022 / Accepted: 18 January 2023 / Published online: 31 January 2023

Abstract

The changes in crystallization behavior, thermal and some physical properties of lead borate glasses with the addition of Al_2O_3, ZnO and TiO_2 have been investigated through Fourier-transform infrared spectroscopy, X-ray diffractometry, dilatometry and differential thermal analysis. Differential thermal and X-ray diffraction analyses showed that the addition of TiO_2 leads to an increase in the crystallization capacity of the $70PbO–30B_2O_3$ glass, while Al_2O_3 and ZnO mainly inhibit the formation of crystalline phases. Fourier-transform infrared spectroscopy results showed that the addition of Al_2O_3 to the lead borate glass matrix leads to a decrease in the number of bridging oxygen atoms and causes a significant decrease in the proportion of tetrahedral borate units. According to dilatometry data, the glass transition temperature (280–320 °C) and dilatometric softening point (305–345 °C) increase, while the thermal expansion coefficient (12.0–9.6 ppm/°C) decreases with equimolar substitution of PbO by Al_2O_3, ZnO or TiO_2. Some physical properties (density, molar volume, and volume resistivity) of the glasses were also estimated.

Introduction

Low-melting glasses based on the lead borate system have a wide range of applications in many fields, including electrical engineering, electronics, nuclear and solar energy, among many others [1–3]. Compared with other oxide systems, lead borate glasses have a number of attractive properties, such as low-melting points, wide glass-formation region [4], good radiation shielding for γ-rays [5], high refractive index and chemical durability [6, 7], and are considered as a basis for manufacturing various protective and decorative coatings, sealing glasses, semiconductor and acousto-optic devices, and as a potential material for radioactive waste immobilization [6–10].

Many studies have shown that lead borate glasses constitute an attractive system for studying the structure-composition-property relationships of glasses [2–5, 8, 9, 11]. The interest in this glass system is primarily due to the fact that PbO is not a classical glass former, but due to the high polarizability and the low field strength of Pb^{2+} ions, in the presence of conventional glass former such as B_2O_3, it may build a glass network of PbO_n polyhedra [11]. Depending on the content of lead oxide in the borate network, it can act as both a glass former and a modifier, positively affecting the glass-forming ability, structure, and properties of glass. The lowest-melting eutectic in the $PbO–B_2O_3$ system with a melting point of 493 °C contains 70% PbO and 30% B_2O_3 [12]. Despite the low melting point of this glass, it cannot be used as a sealing and solder glass, primarily due to its rapid devitrification. Increasing the thermal resistance of glass to devitrification is often achieved by increasing the number of components [3]. The addition of a small amount of intermediate oxides, especially Al_2O_3, TiO_2 and ZnO, to heavy metal borate glasses causes competition between cations to compensate for the charge of borate units, thereby changing the structure, thermal, optical, electrical and other properties critically dependent on the proportion of tetrahedral boron units [13–16]. This is expected to stabilize the glass network structure and increase the thermal stability of the glass to devitrification, henceforth making eutectic lead borate glass suitable candidates for practical applications as protective and decorative coatings, non-crystallizing low-melting sealing and solder glasses.

Therefore, the aim of this work was to study the influence of the addition of Al_2O_3, ZnO and TiO_2 on the changes in crystallization behavior, thermal, and some physical

✉ Yu. S. Hordieiev
yuriihordieiev@gmail.com

[1] Department of Ceramics, Glass and Construction Materials, Ukrainian State University of Chemical Technology, 8 Gagarin Avenue, Dnipro 49005, Ukraine

properties of 70PbO–30B_2O_3 glass using Fourier-transform infrared spectroscopy, X-ray diffractometry, dilatometry and differential thermal analysis.

Materials and methods

The details of the batch composition of the investigated glasses with the corresponding label are given in Table 1. Reagent grade chemicals of Pb_3O_4, H_3BO_3, TiO_2, Al_2O_3 and ZnO were used as starting raw materials. The glass batches were prepared by mixing an appropriate mole fraction of the desired oxide ingredients in an agate mortar with a pestle to ensure complete homogeneity. An electric furnace with silicon carbide elements was utilized to heat the batches in 50 ml platinum crucibles at 900 °C for 30 min in an air atmosphere. The homogeneous melts were quickly cast onto a preheated stainless-steel mold. The glass samples were annealed in a muffle furnace at 260 °C for 3 h and then slowly cooled to room temperature to avoid internal stress.

The glass samples were ground to powder with the use of an agate mortar and pestle. The glass powders were sieved through a set of standard sieves, and the fraction that passed the 270 mesh sieve (53 μm) and retained by the 325 mesh sieve (45 μm) was used for differential thermal analysis. Thermal properties for the investigated glasses were measured by differential thermal analysis (DTA) at a constant heating rate of 5 °C/min (Derivatograf Q-1500D) from room temperature to 800 °C in an air atmosphere. The reference substance was high-purity alumina powder, and the temperature error was ± 5 °C. In this work, the onset of the endothermic peak on the DTA curves was taken as T_g. The temperature difference between the glass transition (T_g) and the first exothermic peak (T_c), indicating a measure of the thermal stability (ΔT) against crystallization, was calculated [17]. Higher values of ΔT indicate better stability against crystallization [17].

In order to determine the crystalline phase corresponding to each exothermic peak in the DTA curves, the glass powder was subjected to heat treatment at the crystallization temperature (T_c) in the air for 5 h. Crystalline phases precipitated during heat treatment were identified by X-ray diffractometer DRON-3 M using Co-K_α radiation in the $10 < 2\Theta < 90$ range. The FTIR spectra of the glasses were recorded in the 1600–400 cm^{-1} region using the KBr pellet technique (Thermo Nicolet Avatar 370 FTIR Spectrometer).

The thermal expansion coefficient (TEC), glass transition temperature (T_g), and dilatometric softening point (T_d) of the glass samples were determined using a dilatometer (Dilatometer1300 L, Italy) at a heating rate of 3 °C/min. The TEC value was calculated between 20 and 200 °C, and repeated measurements indicated the thermal expansion coefficient with an error of ± 0.2 ppm/°C. The results of the dilatometry

Table 1 Chemical composition (mol%) and values of the characteristic temperatures (T_g, T_d, T_c, ΔT), thermal expansion coefficient (TEC), density (ρ), molar volume (V_m) and volume resistivity ($\lg\rho$) of the investigated glasses

Sample name	Glass composition (mol%)					DTA			Dilatometry			ρ, (g/cm^3)	V_m, (cm^3/mol)	$\lg\rho_{150\ °C}$ (Ω cm)
	PbO	B_2O_3	Al_2O_3	TiO_2	ZnO	T_g, (°C)	T_c, (°C)	ΔT, (°C)	T_g, (°C)	T_d, (°C)	TEC, (ppm/°C)			
PbB	70	30	0	0	0	275	360	85	280	305	12.0	6.85	25.86	10.93
PbBAl2.5	67.5	30	2.5	0	0	280	395	115	280	310	11.2	6.60	26.38	10.98
PbBAl5	65	30	5	0	0	290	–	–	290	320	10.7	6.41	26.69	11.04
PbBAl7.5	62.5	30	7.5	0	0	305	–	–	300	335	10.2	6.20	27.10	11.11
PbBAl10	60	30	10	0	0	310	–	–	310	345	9.6	6.03	27.36	11.27
PbBTi2.5	67.5	30	0	2.5	0	285	395	110	285	315	11.7	6.74	25.75	10.99
PbBTi5	65	30	0	5	0	300	410	110	295	320	11.4	6.65	25.56	11.07
PbBTi7.5	62.5	30	0	7.5	0	310	425	115	310	335	10.9	6.58	25.29	11.14
PbBTi10	60	30	0	10	0	315	440	125	320	345	10.6	6.46	25.20	11.26
PbBZn2.5	67.5	30	0	0	2.5	275	410	135	280	310	11.7	6.79	25.56	10.97
PbBZn5	65	30	0	0	5	285	435	150	290	310	11.4	6.74	25.23	11.01
PbBZn7.5	62.5	30	0	0	7.5	290	450	160	295	315	11.2	6.67	24.96	11.12
PbBZn10	60	30	0	0	10	295	480	185	300	315	11.0	6.60	24.69	11.27

analysis are presented in Table 1. The density of the glasses was determined at room temperature by the Archimedes principle using distilled water as the immersion liquid and a digital balance with 10^{-4} g sensitivity. The weight of each glass sample was measured three times, and an average was taken to minimize the sources of error. The volume resistivity of the investigated glasses was measured on flat-parallel plates in a cell with graphite electrodes in the temperature range of 100–200 °C at a heating rate of 5 °/min using the teraohmmeter E6-13A.

Results and discussion

All glasses obtained after melting at 900 °C were transparent and bubble-free. The amorphous nature of the glass samples was checked by X-ray diffraction analysis, which showed the absence of a crystallization peak and the presence of a broad halo around $2\theta = 33°$, which is typical for a fully amorphous structure.

The influence of Al_2O_3, ZnO and TiO_2 on the thermal behavior of lead borate glasses was studied by conducting a detailed differential thermal analysis. DTA curves of fine powders of glass samples in the temperature range of 200–600 °C are shown in Fig. 1. As shown in Fig. 1, each curve is characterized by endothermic and exothermic peaks corresponding to the glass transition temperature and crystallization temperature, respectively. The thermal properties measured by DTA are presented in Table 1. With the addition of intermediate oxides to lead borate glass and increasing their content, the glass transition temperature increased from 280 to 310 °C for glasses containing Al_2O_3, from 285 to 315 °C for glasses containing TiO_2, and from 275 to 295 °C for glasses containing ZnO. This increase in T_g with the addition of intermediate oxides may be due to one or more factors: (1) an increase in cross-linking density and bonding strength of the structure due to the formation of RO_4 or RO_6 structural units in the glass framework [15–19]; (2) reducing the atomic mobility in the melt [20]; and (3) distortion of the glass structure with the formation of the three-dimensional (3D) network of B–O–R linkages [19–21]. The observed increase in T_g and ΔT upon equimolar substitution of PbO by Al_2O_3 or TiO_2 is probably due to the substitution of the weaker and more flexible Pb–O bonds (101 kJ/mol) by the strong and rigid Al–O (377 kJ/mol) and Ti–O (305 kJ/mol) bonds [22]. In the case of PbBZn glass samples, adding ZnO increases the glasses' stability against crystallization, while the glass transition temperature values change by only 20 degrees. The addition of ZnO or TiO_2 into the $70PbO–30B_2O_3$ glass composition leads to an increase in the crystallization temperature and a change in the shape of the exothermic peak. The above results show that additions of Al_2O_3, ZnO, or TiO_2 affect the glass structure and crystallization process of lead borate glass.

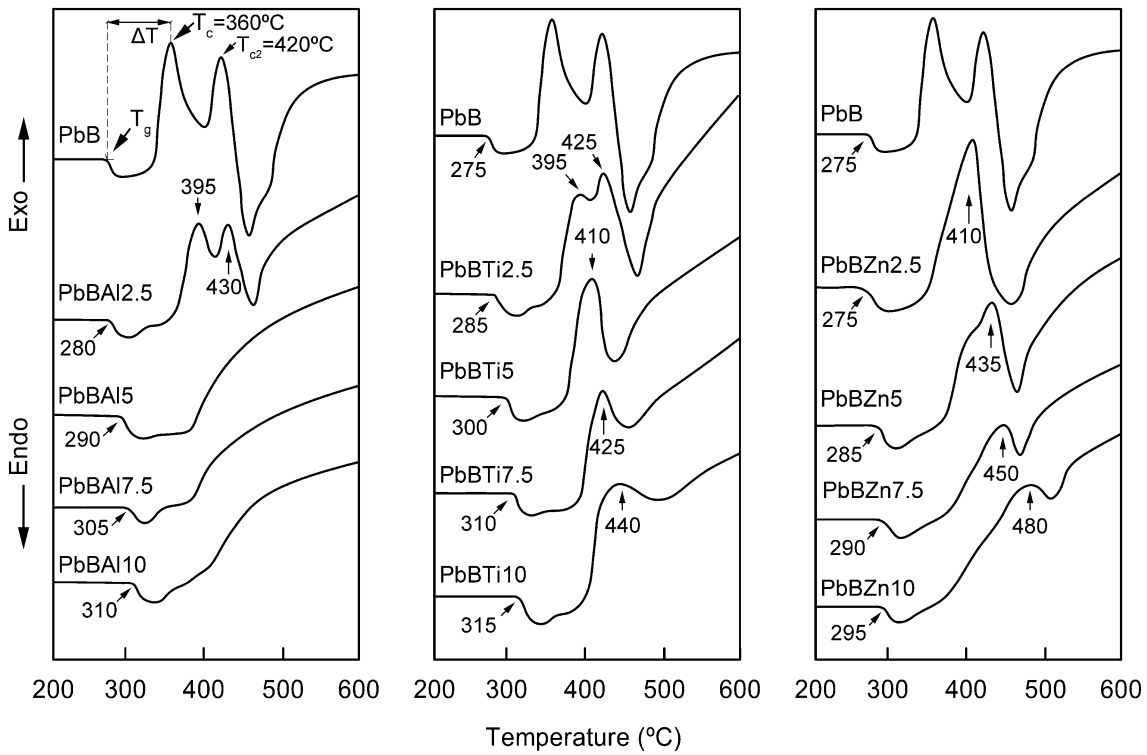

Fig. 1 DTA curves of fine powders of glass samples

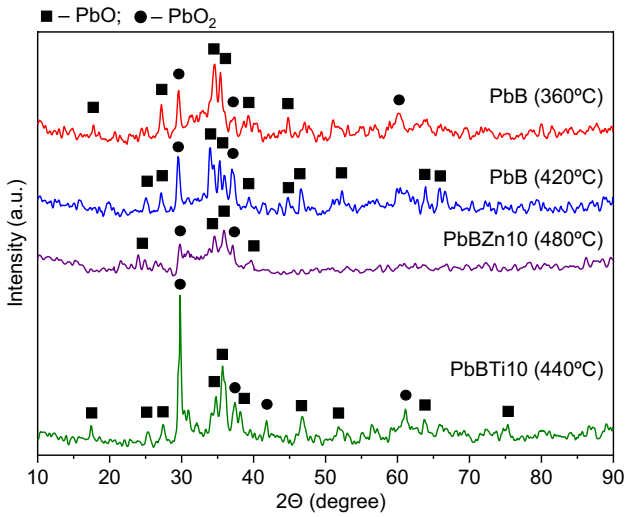

Fig. 2 X-ray diffraction patterns of glass powders heat treated at the crystallization temperature for 5 h

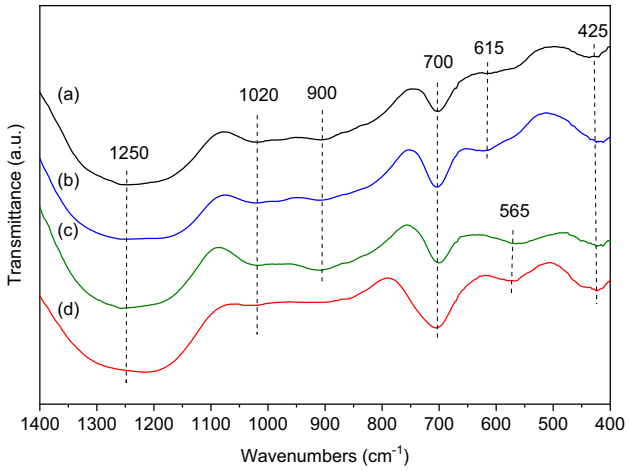

Fig. 3 FTIR spectra of glass samples: **a** PbB, **b** PbBZn10, **c** PbBTi10 and **d** PbBAl10

The crystallization temperatures, determined by DTA, were 360 and 420 °C for PbB, 480 °C for PbBZn5, and 440 °C for PbBTi5. Figure 2 shows the corresponding X-ray diffraction patterns of glass powders after sintering at the crystallization temperature. The X-ray diffraction patterns of all the heat-treated glasses exhibit the formation of PbO (PDF #00-038-1477) and PbO_2 (PDF #00-025-0447) phases identified using powder diffraction files. The intensity of the diffraction peaks of the main crystalline phases precipitated in the glass matrix is significantly reduced with the addition of ZnO into the composition of the base glass. The amounts of the PbO_2 crystalline phase increased with the addition of TiO_2 into the composition of the lead borate glass. It is well-known that TiO_2 is a nucleating agent in borate and borosilicate glasses [17, 19]. The results mentioned above confirmed that TiO_2 acts as a nucleating agent that promotes the crystallization of the base glass, while Al_2O_3 and ZnO mainly inhibit the formation of crystalline phases.

Fourier-transform infrared spectroscopy (FTIR) is a powerful tool for understanding how the local structure of glass changes due to its composition. The influence of Al_2O_3, ZnO and TiO_2 on the structural properties of $70PbO–30B_2O_3$ glass was investigated by detecting FTIR spectra (Fig. 3) in the range 1400–400 cm^{-1}. The broad band observed at 1100–1400 cm^{-1} centered at ~ 1250 cm^{-1} is attributed to stretching vibrations of BO_3 units with non-bridging oxygens (NBOs) [4, 23–25]. Its relative area increases, and the center shifts towards slightly lower wavenumbers with adding Al_2O_3 into the $70PbO–30B_2O_3$ glass composition. Incorporating Al_2O_3 into the glass network at the expense of PbO injects additional oxygen into the structure and forms more BO_3 structural units with NBOs. The absorption bands in the range 800–1100 cm^{-1} are due to the stretching vibration of BO_4 structural units [4, 23–25]. A new band has been observed at 565 cm^{-1} in glass samples PbBTi10 and PbBAl10, which is due to the vibration of TiO_6 [15] and AlO_6 [25, 26] structural units, respectively. The decrease in BO_4 units, increase in BO_3 structural units with NBOs, and the formation of TiO_6 and AlO_6 units in the investigated glasses are probably due to the transformation of TiO_4 and AlO_4 tetrahedra to TiO_6 and AlO_6 octahedra, respectively, by converting BO_4 units to BO_3 units. The strong absorption band centered around 700 cm^{-1} is assumed to be due to the combined vibration of PbO_4 units and the bending vibration of B–O–B in BO_3 triangles [8, 27]. The absorption band centered at 600 cm^{-1} in glass samples PbB and PbBZn10 can be assigned to the bending vibration of B–O–Pb and B–O–Zn linkages in the bridge connection of BO_3 and BO_4 units [27]. Low-frequency bands observed at $\leq$ 450 cm^{-1} are usually attributed to vibrations of metal ions relative to their network sites [28]. In this study, the absorption band at around 425 cm^{-1} can be attributed to the vibration of Pb^{2+}, Ti^{4+}, Al^{3+}, and Zn^{2+} ions.

It is well known that the nature and concentration of the oxides in the composition of glasses substantially determine the thermal and physical properties of oxide glasses [12–15]. The thermal and physical properties of the investigated glasses were investigated by measuring the volume resistivity, thermal expansion coefficient, glass transition temperature, dilatometric softening point, density, and calculating the molar volume values. The obtained values are given in Table 1. At the temperature of 150 °C, the volume resistivity of the investigated glasses is in the range of 10^{10}–10^{12} Ω·cm. The volume resistivity increases with the inclusion of Al_2O_3, ZnO and TiO_2 into the glass network at the expense of PbO. Since Pb^{2+} ions can be considered the dominant charge carriers in lead borate glasses, such

a change in volume resistivity is expected [29]. The equimolar substitution of PbO by Al_2O_3, ZnO or TiO_2 leads to an increase in volume resistivity due to the more compact arrangement of structural groups, resulting in a reduction in the space in which conductive ions can move. The density of investigated glasses decreases with the substitution of PbO by Al_2O_3, ZnO or TiO_2. This behavior is attributed to the relatively lower molecular weight of Al_2O_3 (101.96 g/mol), ZnO (81.39 g/mol) and TiO_2 (79.87 g/mol) than PbO (223.2 g/mol). The molar volume decreases with increasing TiO_2 and ZnO content and increases with increasing Al_2O_3 content. The increase in the molar volume with an increase in the Al_2O_3 content may be due to the formation of non-bridging oxygen and the expansion of the structure of the network of the lead borate glass. The decrease in molar volume with the inclusion of ZnO or TiO_2 into the lead borate glass network can be attributed to a decrease in bond length or interatomic spacing among the atoms of the glass network, which causes the compaction of the structure [30]. It can be seen from the dilatometry results that the glass transition temperature (280–320 °C) and dilatometric softening point (305–345 °C) increased, while the thermal expansion coefficient (9.6–12.0 ppm/°C) decreased with equimolar substitution of PbO by Al_2O_3, ZnO or TiO_2. The observed decrease in TEC values and an increase in T_g and T_d values can be attributed to the substitution of the weaker Pb–O bonds by the stronger Zn–O, Al–O and Ti–O bonds.

Conclusions

In the present study, the influence of Al_2O_3, ZnO and TiO_2 was investigated on the crystallization behavior, thermal, and some physical properties of lead borate glasses. Fourier-transform infrared spectroscopy results showed that the network of the investigated glasses consists mainly of BO_3, BO_4, and PbO_4 structural units. The depolymerization of the glass network increases with the increasing content of Al_2O_3. Differential thermal analysis and X-ray diffraction analysis showed that the addition of TiO_2 leads to an increase in the crystallization capacity of the base glass, while Al_2O_3 and ZnO mainly inhibit the formation of crystalline phases. The equimolar substitution of PbO by Al_2O_3, ZnO or TiO_2 results in a decrease in density and thermal expansion coefficient and an increase in glass transition temperature, dilatometric softening point, glass stability and volume resistivity of the investigated glasses. The decrease in density is due to the relatively lower molecular weight of Al_2O_3, ZnO and TiO_2 than PbO. The observed decrease in TEC values and an increase in T_g, T_d and ΔT values are due to the substitution of the weaker and more flexible Pb–O bonds by the strong and rigid Zn–O, Al–O and Ti–O bonds, which in turn leads to an increase in bonding strength of structural groups in the glass matrix.

Acknowledgments The authors gratefully acknowledge the financial support from the Ministry of Education and Science of Ukraine.

Author contributions YSH wrote the manuscript, conceived and designed the experiments, performed experimental work; AVZ provided the reagents and assisted in experimental work. All authors read and approved the final manuscript.

Funding This work was supported by the Ministry of Education and Science of Ukraine.

Data availability The data that support the findings of this study are available from the corresponding author on reasonable request.

Declarations

Competing interest The authors declare that they have no conflict of interest. The authors declare that they have no known competing financial interests or personal relationships that could have influenced the work reported in this paper.

Ethical approval Not applicable.

Consent to participate Not applicable.

Consent for publication Not applicable.

References

1. H. Li, H. Tong, J. Zhang, G. Li, Y. Yang, C. Liu, H. Li, X. Yuan, J. Electron. Mater. **49**, 5422–5429 (2020). https://doi.org/10.1007/s11664-020-08281-w
2. D. Singh, K. Singh, G. Singh, Manupriya, S. Mohan, M. Arora, and G. Sharma, J. Phys. Condens. Matter **20**, 075228 (2008). https://doi.org/10.1088/0953-8984/20/7/075228
3. V.I. Goleus, Y.S. Hordieiev, A.V. Nosenko, Vopr. Khimii i Khimicheskoi Tekhnol. **4**, 92–96 (2018)
4. Y. Cheng, H. Xiao, W. Guo, W. Guo, Ceram. Int. **33**, 1341–1347 (2007). https://doi.org/10.1016/j.ceramint.2006.04.025
5. H. Singh, K. Singh, L. Gerward, K. Singh, H.S. Sahota, R. Nathuram, Nucl. Instrum. Methods Phys. Res. B **207**, 257–262 (2003). https://doi.org/10.1016/s0168-583x(03)00462-2
6. A.V. Nosenko, Y.S. Hordieiev, V.I. Goleus, Vopr. Khimii i Khimicheskoi Tekhnol. **1**, 87–91 (2018)
7. O. Krupych, I. Martynyuk-Lototska, A. Say, V. Boyko, V. Goleus, Y. Hordieiev, R. Vlokh, Ukr. J. Phys. Opt. **21**, 47–56 (2020). https://doi.org/10.3116/16091833/21/1/47/2020
8. C. Erdogan, M. Bengisu, S.A. Erenturk, J. Nucl. Mater. **445**, 154–164 (2014). https://doi.org/10.1016/j.jnucmat.2013.10.025
9. B.V. Padlyak, I.I. Kindrat, A. Drzewiecki, V.I. Goleus, Y.S. Hordieiev, J. Non-Cryst. Solids **557**, 120631 (2021). https://doi.org/10.1016/j.jnoncrysol.2020.120631
10. N.M. Bobkova, Glass Ceram. **66**, 206–209 (2009). https://doi.org/10.1007/s10717-009-9170-2
11. B.V. Padlyak, I.I. Kindrat, Y.O. Kulyk, S.I. Mudry, A. Drzewiecki, Y.S. Hordieiev, V.I. Goleus, R. Lisiecki, Mater. Sci. Eng. B Solid State Mater. Adv. Technol. **278**, 115655 (2022). https://doi.org/10.1016/j.mseb.2022.115655

12. R.F. Geller, E.N. Bunting, J. Res. Natl. Bur. Stand. **18**, 585 (1937)
13. A. Saini, A. Khanna, V.K. Michaelis, S. Kroeker, F. González, D. Hernández, J. Non Cryst. Solids. **355**, 2323–2332 (2009). https://doi.org/10.1016/j.jnoncrysol.2009.08.006
14. J. Singh, G.P. Singh, P. Kaur, T. Singh, S. Bhatia, R. Kaur, D.P. Singh, Acta Phys. Pol. A. **142**, 195–200 (2022). https://doi.org/10.12693/aphyspola.142.195
15. H. Doweidar, K. El-Egili, R. Ramadan, M. Al-Zaibani, J. Non Cryst. Solids. **466–467**, 37–44 (2017). https://doi.org/10.1016/j.jnoncrysol.2017.03.040
16. A.J. Lere-Adams, N. Stone-Weiss, D.L. Bollinger, J.S. McCloy, MRS Adv. **7**, 90 (2022). https://doi.org/10.1557/s43580-022-00219-0
17. Q. Chen, Q. Wang, Q. Ma, H. Wang, J. Non Cryst. Solids. **464**, 14 (2017). https://doi.org/10.1016/j.jnoncrysol.2017.03.015
18. B.V. Padlyak, I.I. Kindrat, Y.O. Kulyk, Y.S. Hordieiev, V.I. Goleus, R. Lisiecki, Mater. Res. Bull. **158**, 112071 (2023). https://doi.org/10.1016/j.materresbull.2022.112071
19. G.N. Raju, Y. Gandhi, N.S. Rao, N. Veeraiah, Solid State Commun. **139**, 64–69 (2006). https://doi.org/10.1016/j.ssc.2006.04.032
20. H. Es-soufi, L. Bih, J. Electron. Mater. **51**, 2528–2544 (2022). https://doi.org/10.1007/s11664-022-09497-8
21. G.P. Singh, J. Singh, P. Kaur, T. Singh, R. Kaur, S. Kaur, D.P. Singh, J. Alloys Compd. **885**, 160939 (2021). https://doi.org/10.1016/j.jallcom.2021.160939
22. V. Dimitrov, T. Komatsu, J. Univ. Chem. Technol. Metall. **45**, 219–250 (2010)
23. S. Baccaro, Monika, G. Sharma, K.S. Thind, D. Singh, A. Cecillia, Nucl. Instrum. Methods Phys. Res. B. **260**, 613–618 (2007). https://doi.org/10.1016/j.nimb.2007.04.214.
24. P.S. Prasad, B.V. Raghavaiah, R.B. Rao, C. Laxmikanth, N. Veeraiah, Solid State Commun. **132**, 235–240 (2004). https://doi.org/10.1016/j.ssc.2004.07.042
25. B.A. Rao, Y.R. Rao, IOP Conf. Ser.: Mater. Sci. Eng. **73**, 012095–012098 (2015). https://doi.org/10.1088/1757-899X/73/1/012095
26. H. Gui, C. Li, C. Lin, Q. Zhang, Z. Luo, L. Han, J. Liu, T. Liu, A. Lu, J. Eur. Ceram. Soc. **39**, 1397–1410 (2019). https://doi.org/10.1016/j.jeurceramsoc.2018.10.002
27. E. Mansour, J. Non Cryst. Solids **358**, 454–460 (2012). https://doi.org/10.1016/j.jnoncrysol.2011.10.037
28. H. Doweidar, Y.B. Saddeek, J. Non Cryst. Solids **356**, 1452–1457 (2010). https://doi.org/10.1016/j.jnoncrysol.2010.04.036
29. C.A. Gressler, J.E. Shelby, J. Appl. Phys. **66**, 1127–1131 (1989). https://doi.org/10.1063/1.343452
30. G.P. Singh, S. Kaur, P. Kaur, D.P. Singh, Phys. B Condens. Matter. **407**, 1250–1255 (2012). https://doi.org/10.1016/j.physb.2012.01.114